

# Electrochemistry and Characterization of Some Organic Molecules at “Microsize” Conducting Polymer Electrodes

Ahmed Galal<sup>†\*</sup>

Department of Chemistry, Faculty of Science, United Arab Emirates University, P.O. Box 17551, Al-Ain, United Arab Emirates

<sup>†</sup>On leave from the Department of Chemistry, Faculty of Science, University of Cairo, Giza, Egypt

Received: July 28, 1997

Final version: December 15, 1997

## Abstract

Poly(3-methylthiophene) is electrochemically deposited on platinum microsize substrate. Two methods are used for the electropolymerization including applying constant potential of 1.65 V to 1.75 V, or cycling the working electrode between two potential limits from -0.2 V to 1.65–1.80 V (vs. Ag/AgCl). The resulting conducting polymer electrode is used for the determination of some organic molecules of biological interest. The resolution of the voltammetric peaks obtained for the determination of a mixture of three components analyte is a function of the method used for electrodeposition of the polymer film. The electrochemical data obtained at the microsize conducting polymer electrode are compared to those obtained at “conventional”-size polymer electrodes. The morphology of the microsize polymer electrode is examined using scanning electron microscopy. The data suggest great promise for using microsize polymer electrodes as electrochemical sensor for biomedical applications.

**Keywords:** Microelectrodes, Sensors, Conducting polymers, Electrochemistry, Biological molecules

*This work is dedicated to Prof. Harry B. Mark, Jr. on the occasion of his 60<sup>th</sup> birthday.*

## 1. Introduction

Conducting polymers represent a class of materials with electronic conductivity [1]. The most important polymers of this class are poly(acetylene), poly(pyrrole), poly(thiophene), poly(*p*-phenylene), poly(aniline), and their derivatives. The first successful attempt for the electrochemical polymerization appeared in the 1950s by the efforts of Funt et al. [2]. However, the first electronically conducting polymeric systems with conjugated double bonds were synthesized by Dall’Olio et al. in the 1960s [3]. Moreover, it was only in the late 1970s that Heeger et al. [4] and Diaz et al. [5] discovered that these materials would undergo chemical and electrochemical redox transitions to yield polymers with relatively high intrinsic electronic conductivities.

These materials are now competing with the classical surfaces such as metals and carbon in electrochemical applications [6, 7]. Some aspects making modified electrodes look attractive as electrochemical tools are the possibility of preconcentrating the analyte near or at the electrode surface, the high selective nature of the modified surface and its remarkable sensitivity. The implementation of the above properties along with some specific catalytic activity will result in minimizing high background currents by the suppression of competing redox reactions. Fouling of the electrode surface has long been a serious problem in electrochemical determinations of many organic compounds. Polymer coating of the surface of the electrode substrate helped to alleviate this problem [8].

On the other hand, metal and carbon electrodes with extremely small dimensions, in the  $\mu\text{m}$  or submicron range, have been used for voltammetric measurements and were developed for biological and medical research [9]. The work of Fleischmann et al. [10] revealed that a decrease in the surface area of the electrode not only affects quantitative changes, but also results in unusual qualitative effects. One major advantage of microelectrodes is that the expansion of the inherently small diffusion layer on the time scale of the experiment is greater than the characteristic dimensions of the electrode. In the case of the frequently employed disk electrode such a characteristic is its radius. Relatively large diffusion layers develop a few seconds

after the current starts passing through electrodes with dimensions  $<20\ \mu\text{m}$ . The hemi-spherical diffusion (versus a planar one for conventional electrodes) leads to higher flux of the electroactive species. The mass transport coefficient  $m$ , which is a measure of the rate of transport of electroactive species in the diffusion layer is given by:

$$m = \frac{D}{r} \quad (1)$$

where  $D$  is the diffusion coefficient, and  $r$  is the electrode radius. As a result, the diffusion rate is exceptionally large as the electrode dimension decreases. Moreover, the current density at small-size electrodes is relatively large (compared to conventional electrodes) and results in considerable increase in the ratio of the faradic to the capacitive currents. Thus, the property of enhanced fast mass transport was anticipated for the development of in vivo fast microvoltammetric sensors by minimizing the electrocatalytic reaction between ascorbic acid and dopamine [11]. With the help of a fast potentiostat and the use of ultramicroelectrodes, it was possible to obtain fast kinetic information about the redox behavior of conducting polymer films [12] and their electropolymerization mechanism [13]. It was also found, that, ultramicroelectrodes coated with poly(aniline) [14] could be switched between its redox states more rapidly than has previously reported.

In this work we have electrochemically deposited poly(3-methylthiophene) on a Pt microelectrode. The resulting micropolymer electrode was used as electrochemical sensor for the determination of some organic molecules of biological interest. The electrochemical characteristics of the micropolymer electrode were determined and compared to “conventional-size” polymer electrode. The surface morphology of the polymer film was examined using scanning electron microscopy (SEM). The properties of the microsize and the catalytic property of the polymer electrode are anticipated and suggest the potential of this sensor in several applications. The sensor is useful when microliter biological samples are available, when fouling of the sensor surface is expected and when improved resolution of a multicomponent system is desirable.

## 2. Experimental

### 2.1. Chemicals and Materials

All chemicals used were reagent grade. Epinephrine, norepinephrine and tetrabutyl-ammonium tetrafluoroborate (TBATFB) were purchased from Fluka (USA). Other chemicals used in this work were obtained from Aldrich (USA). 3-Methylthiophene was used as the monomer after fractional distillation. Acetonitrile was kept over molecular sieves type A4. Phosphate buffer was prepared by mixing 600 mL  $\text{Na}_2\text{HPO}_4$  (9.470 g/L) and 400 mL  $\text{NaH}_2\text{PO}_4$  (9.208 g/L) containing 4.60 g of NaCl. Aqueous solutions were prepared using distilled water, further purified by a Sybron/Barnstead Pure II system.

### 2.2. Apparatus

Electrochemical polymerization was carried out with a three-electrode system where the working electrode was a platinum disk electrode (surface area  $0.280\text{ cm}^2$  or  $3.14 \times 10^{-10}\text{ cm}^2$ , for the microelectrode). The auxiliary electrode was a  $2 \times 2\text{ cm}^2$  platinum sheet. The electrode was polished using metallurgical papers and alumina-water suspension, sonicated, rinsed with water and dried. All the potential values in this study are referred to a Ag/AgCl electrode (3M KCl).

Electrosynthesis of the polymer films were performed using an EG&G Model 173 potentiostat/galvanostat equipped with an EG&G 179 coulometer (PAR, USA). A BAS 100 equipped with a current amplification unit was used for electropolymerization and electrochemical characterizations. Some experiments were conducted using a CMS 100 electrochemical system (Gamry Instruments Inc. USA). All solutions were deaerated by bubbling argon gas through the electrolytic cell. The polymer film was formed under constant applied potentials or by repeatedly scanning the electrode between two potential limits. Scanning electron microscopy studies were performed with a Cambridge Stereoscan 600 instrument.

## 3. Results and Discussion

### 3.1. Electrode Preparation

The polymer film was formed at the surface of the platinum microelectrode by repeatedly cycling the electrode between the following potential limits:  $-0.12\text{ V}$  and  $1.7\text{ V}$ . Typical cyclic voltammogram of 3-methylthiophene at  $8\text{ }\mu\text{m}$ -diameter platinum electrode using  $100\text{ mV/s}$  scan rate is given in Figure 1. The following conclusions are drawn:

- 3-Methylthiophene is oxidized at  $+1.56\text{ V}$ , to form the corresponding polymer.
- Upon reversing the direction of sweep from the first oxidation wave, a corresponding cathodic wave for the reduction of the polymer film is observed in the region from  $+0.70\text{ V}$  to  $+0.50\text{ V}$ .
- The subsequent anodic sweeps revealed the growth of the polymer film at a lower oxidation potential (ca.  $E_{\text{pa}} + 1.40\text{ V}$ ). The anodic peak potential ( $E_{\text{pa}}$ ) occurring at ca.  $+0.65\text{ V}$  is attributed to the oxidation of the polymer film deposited during subsequent cycles. The formation of a polymer layer over the substrate was indicated by the increase of the current at a potential of about  $1.6\text{ V}$ , i.e., the oxidation potential of the monomer [15]. The data obtained in Figure 1 indicate that the

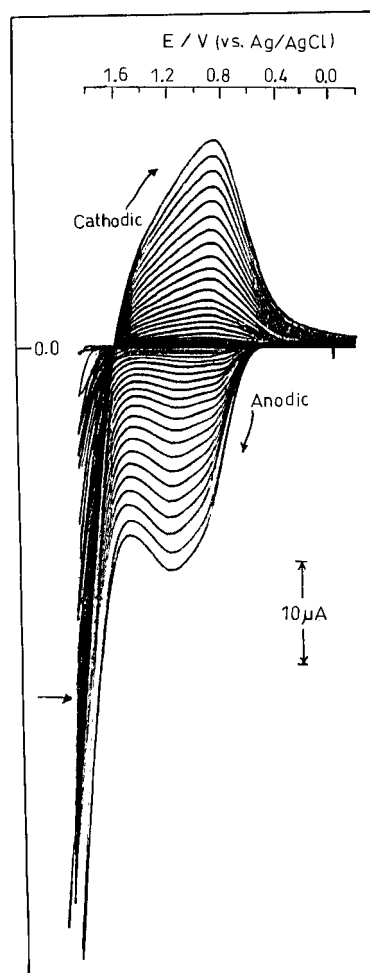


Fig. 1. Repeated cyclic voltammograms of  $0.05\text{ M}$  3-methylthiophene/ $0.05\text{ M}$  tetrabutyl-ammonium tetrafluoroborate in acetonitrile at Pt microelectrode. Scan rate  $100\text{ mV/s}$ .

layer of polymer film formed in each cycle catalyzes the oxidation of the monomer at the following cycle.

Thus, the cyclic voltammogram of 3-methylthiophene at microsize electrode has all the characteristics of an ECE reaction [17]. The limiting current for a spherical electrode is given by

$$i_l = nF\pi r^2 Dc \left[ \frac{1}{(\pi Dt)^{1/2}} + \frac{1}{r} \right] \quad (2)$$

All terms in the above equation have the regular meaning. The first term, however, describes the current due to linear diffusion while the second shows the one due to the edge effect. For the microsize electrode, the current is time independent, and the steady state will be reached when the following two conditions are realized:

$$\frac{1}{(\pi Dt)^{1/2}} \ll \frac{1}{r} \quad \text{and} \quad \frac{10}{(\pi Dt)^{1/2}} \ll \frac{1}{r} \quad (3)$$

At high scan rates the cyclic voltammograms obtained at those electrodes are wave-shaped. As the scan rate decreases the voltammograms become sigmoidal in shape. Figure 2 shows the cyclic voltammogram obtained at  $8\text{ }\mu\text{m}$  Pt electrode for  $5\text{ mM}$  catechol in phosphate buffer (pH 6.9) with a scan rate of  $100\text{ mV/s}$ . This result is comparable to the steady-state voltammograms at rotating disk electrodes. The similarity is a result of the high diffusion due to mass transport rate when compared to rotating disk electrodes [16]. On the other hand, the data depicted in Figure 1 showed that the anodic peak potential appearing at ca.  $+0.6\text{ V}$

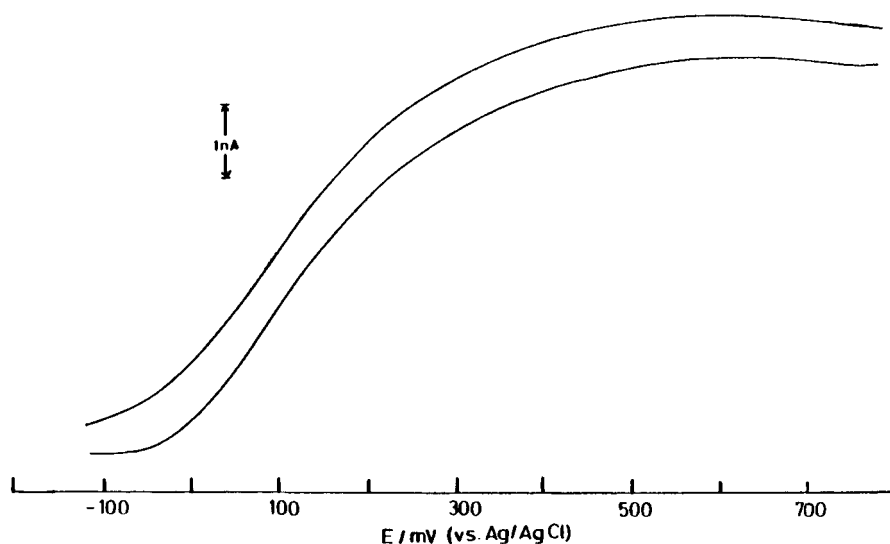


Fig. 2. Cyclic voltammogram of 5 mM catechol in phosphate buffer (pH 6.9) at Pt microelectrode. Scan rate 100 mV/s.

correspond to the oxidation of the polymer film while the cathodic peak occurring at ca. +0.55 V can be attributed to the reversible process due to the film formation (at +1.40 V) and to the reduction of the polymer. The film thickness was controlled by the number of cycle scans applied to the electrode.

### 3.2. Electrochemical Characterization of some Organic Molecules of Biological Interest at the Microsize Polymer Electrode

Poly(3-methylthiophene) was grown on Pt microelectrode substrate by repeatedly cycling the electrode as previously described for ten scans. The repeated cyclic voltammogram of the resulting electrode in phosphate buffer (pH 6.9) containing 5 mM  $K_3[Fe(CN)_6]$  is given in Figure 3. The following conclusions are drawn:

- The anodic and cathodic peak potentials are well defined as depicted in Figure 3, although the background current is not subtracted (curve a).
- The anodic and cathodic peak potentials appear at +0.25 V and +0.17 V, respectively.
- The peak separation is ca. 80 mV.

Moreover, it can be noticed from Figure 3 that the contribution of the nonlinear (hemispherical) diffusion is not significant. Therefore, it is possible to apply the Randles-Sevcik equation to this electrode [16]. Figure 3 shows also that repeatedly cycling the polymer microelectrode in the same electrolyte did not result in the disappearance of current signal. This proves that the conducting polymer microelectrode overcomes the complication that face film-based sensors which are the change in stability, the lack of continuous activity of the film and the signal attenuation due to surface fouling.

The sensor application of this conducting polymer microelectrode was implemented by constructing calibration plots obtained for different neurotransmitters using the anodic peak current of the cyclic voltammograms shown in Figure 4A. The calibration plot for hydroquinone in phosphate buffer (pH 6.9) obtained at conducting poly(3-methylthiophene) microelectrode is given in Figure 4B. The slope of the calibration plot was normalized to the electrode surface area showed a value of  $7.4 \text{ A/mM cm}^2$  (correlation coefficient of 0.994). Similar plots for dopamine, catechol, norepinephrine, epinephrine, and *p*-aminophenol were obtained and gave the data

shown in Table 1. In all cases, the poly(3-methylthiophene) film was deposited by repeatedly cycling the ultramicro-platinum substrate between  $-0.12 \text{ V}$  and  $+1.8 \text{ V}$  for ten cycles in 50 mM 3-methylthiophene/100 mM TBATFB in AcN. The electrode was then rinsed thoroughly and cycled between  $-0.5 \text{ V}$  and  $+0.7 \text{ V}$  in different concentrations of hydroquinone in phosphate buffer (pH 6.9) prepared by successive dilutions from a 100 mM analyte stock solution. The results obtained, so far, for polymer

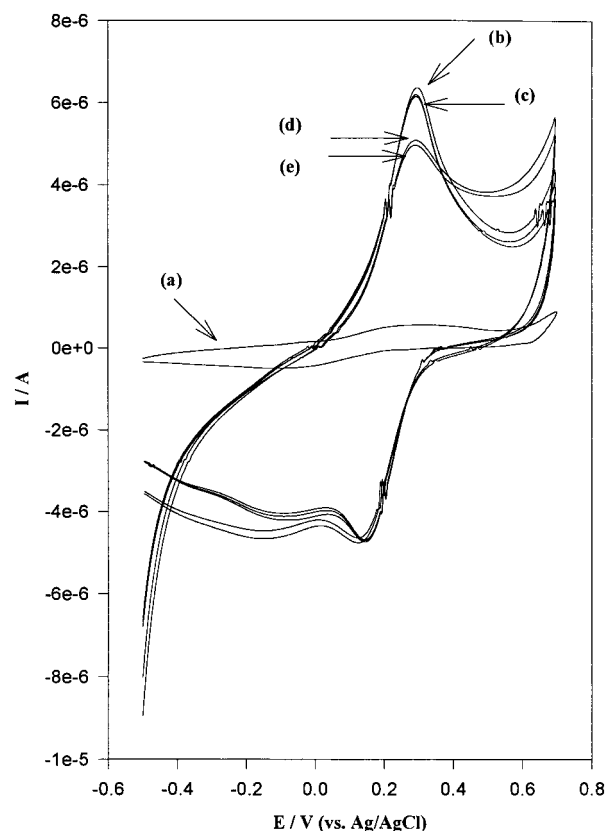


Fig. 3. Repeated cyclic voltammograms of 5 mM  $K_3[Fe(CN)_6]$ /phosphate buffer (pH 6.9) at conducting poly(3methylthiophene) microelectrode. Scan rate 100 mV/s. Polymer electrode formed by repeated cyclic voltammetry. In the absence of ferricyanide (curve a), in the presence of ferricyanide; cycle 1 (curve b), cycles 2 and 3 (curve c), cycle 50 (curve d) and cycle 100 (curve e).

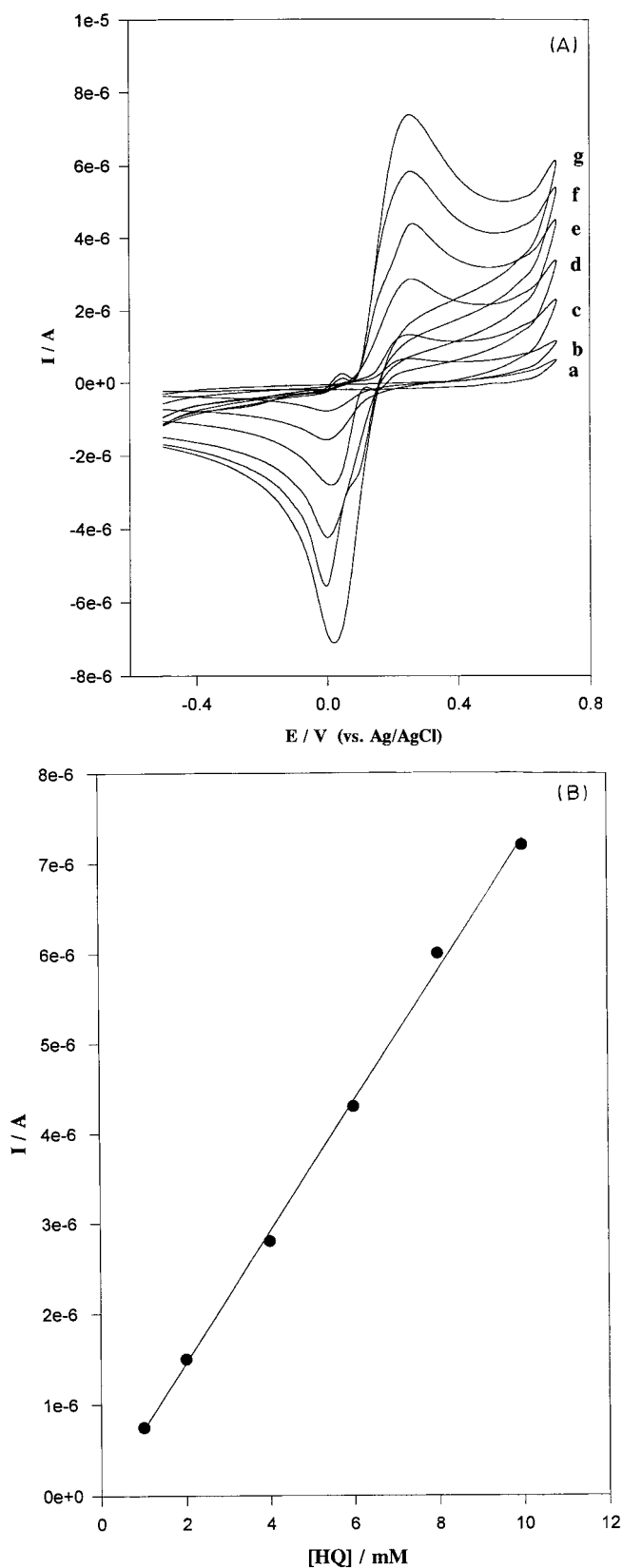


Fig. 4. A) Cyclic voltammograms at conducting poly(3-methylthiophene) micro-electrode in different concentrations of hydroquinone/phosphate buffer (pH 6.9). Background (curve a), 1 (curve b), 2 (curve c), 4 (curve d), 6 (curve e), 8 (curve f), and 10 (curve g) mM hydroquinone, respectively. B) Calibration plot for the determination of hydroquinone at the conducting polymer microelectrode formed as in Figure 3. Data were obtained by measuring the anodic peak current values from the corresponding voltammograms.

Table 1. Calibration plot data for different compounds at PMT microelectrode. Electrolyte: phosphate buffer (pH 6.9)/1–10 mM analyte, data collected from cyclic voltammetric experiments, using 50 mV/s scan rates.

| Compound               | Slopes<br>[A/mM cm <sup>2</sup> ] | Correlation<br>coefficient | Detection limits<br>[mM] |
|------------------------|-----------------------------------|----------------------------|--------------------------|
| Potassium ferricyanide | 7.4                               | 0.994                      | $7.4 \times 10^{-3}$     |
| Dopamine               | 8.2                               | 0.988                      | $8.1 \times 10^{-3}$     |
| Catechol               | 12.4                              | 0.995                      | $6.2 \times 10^{-3}$     |
| Norepinephrine         | 9.5                               | 0.994                      | $5.7 \times 10^{-3}$     |
| Epinephrine            | 7.8                               | 0.996                      | $6.6 \times 10^{-3}$     |
| p-Aminophenol          | 14.1                              | 0.998                      | $3.7 \times 10^{-3}$     |

microelectrodes prove to be superior compared to the substrates. It is also evident that these electrodes can be used repeatedly for the determination of biological samples of relatively low concentrations. An important aspect for this electrode is the fact that the current magnitude obtained is accessible without special amplification.

### 3.3. Multicomponent System Detection

The utility of the conducting polymer microelectrode has been extended towards the analysis of a multicomponent system, involving a mixture of ascorbic acid, *p*-aminophenol, and catechol, in a manner to work with conventional electrodes [18]. The results presented in Figure 5A show very good resolution for the peaks obtained for the determination of a mixture of 1 mM ascorbic acid, *p*-aminophenol, and catechol in 0.1 M phosphate buffer (pH 6.9) using the square wave voltammetric technique. The electrode in Figure 5A was prepared by repeated cyclic voltammetry as described above while that in Figure 5B was prepared by holding the potential of the ultramicro-platinum substrate in 3-methylthiophene/TBATFB electrolyte at +1.7 V for 25 s. A double potential step was applied from 0.0 V to +0.80 V or +1.0 V (vs. Ag/AgCl).

The conducting polymer microelectrode showed considerable resemblance in the electrochemical behavior of the studied electrolytes when compared to the data obtained earlier for conventional polymer electrode [18]. The data of Table 2 showed that for all compounds studied the anodic and cathodic peak potential values were comparable at both electrodes. The effect of changing the scan rate on both anodic and cathodic peak current values at the polymer microelectrode of different compounds showed that the process of charge transfer was under diffusion control. A linear relation was observed between the anodic peak current values plotted versus the square root of the scan rate (not shown).

### 3.4. Effect of the Method Used for Polymer Film Formation

The method used to deposit the polymer film was shown to be critical for the resolution capability of the conducting polymer microelectrode. This observation was not noticed in the case of conventional size electrodes [18]. Figure 5B shows the results obtained for the same mixture of compounds and under similar experimental conditions as those displayed in Figure 5A. The polymer film used in the voltammetric experiment of the data shown in Figure 5B, however, was formed under constant applied potential of 1.7 V for 25 s. The film thickness is 50  $\mu\text{m}$  and 30  $\mu\text{m}$  for the polymer electrodes formed by repeated cycles and applying constant potential for the data displayed in Figures 5A, 6A and 5B, 6B respectively. The film thickness is estimated from the coulometric charge passing during the film formation. As could be noticed from the voltammogram obtained in Figure 5B, the peaks became ill resolved as compared to those depicted in Figure 5A. One possible reason could be attributed to the differences in morphological aspects of the films grown under

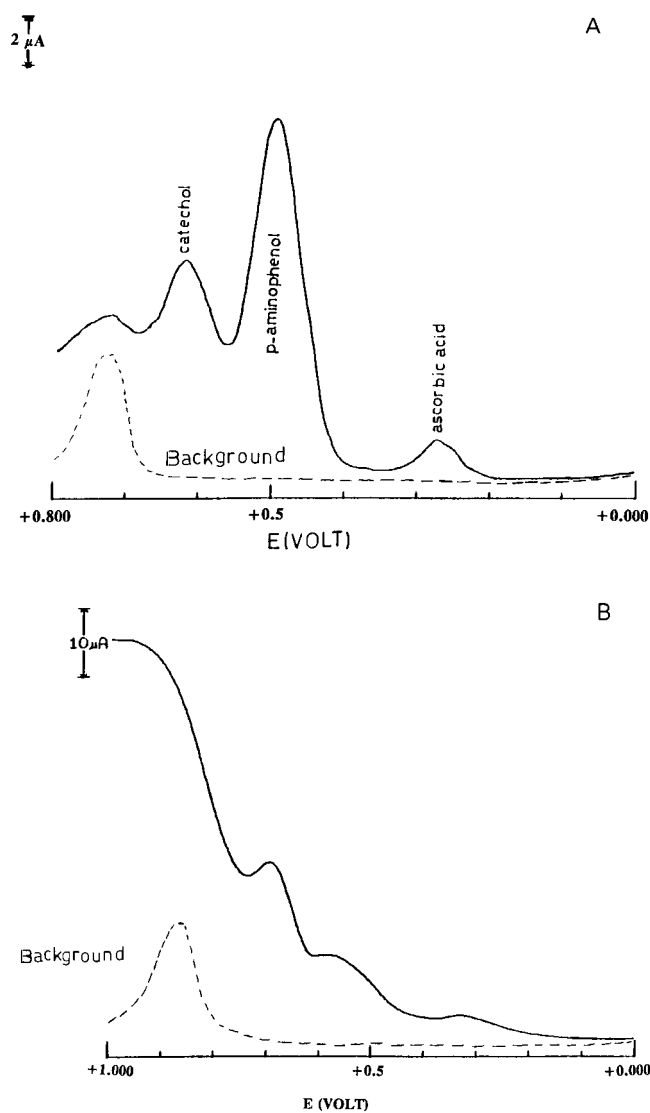


Fig. 5. A) Double potential step square wave voltammogram of a mixture of 1 mM ascorbic acid, *p*-aminophenol, and catechol in phosphate buffer (pH 6.9). Electrode formed by repeated cyclic voltammetry. B) Same as in A), but electrode is formed under constant applied potential condition.

two different conditions. The scanning electron microscopy data confirmed this assumption.

### 3.5. Morphological Structure of Conducting Polymer Microelectrodes

The morphology of conducting poly(heteroarylene)s is found to mainly depend on three parameters: the structure of the monomer, the nature of the dopant, and the thickness of the film grafted on the electrode. These observations are similar to what was reported earlier in the literature [19]. SEM analysis showed that when the poly(3-methylthiophene) films were grafted as thin films, about  $10^2$  to  $10^3$  Å thick, the surface was very homogeneous, regardless of the nature of the polymer or the anion. When the polymer thickness was increased to a few microns, a powdery deposit rather than a smooth film was obtained. The morphological changes could be explained in terms of the structural defects, such as crosslinking,  $\beta$ - versus  $\alpha$ -coupling of the thiophene units, and the reticulation associated with it. The analysis of the inner structure of this class of

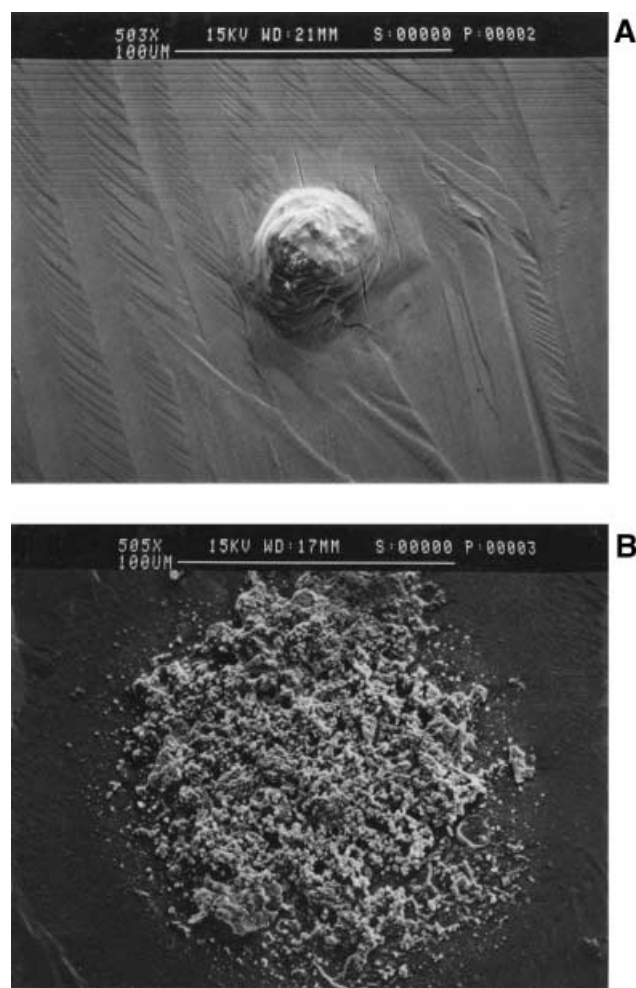


Fig. 6. A) Scanning electron micrograph of conducting polymer microelectrode formed by repeated cyclic voltammetry. B) Same as A), but electrode formed under constant potential condition.

conducting polymers performed by SEM and transmission electron microscopy (TEM) revealed that the “noodle”-like or the fibrillar structure of the polymer films increases with the level of doping [20]. Figure 6 shows the SEM graphs of poly(3-methylthiophene) electrochemically grown on Pt microsize electrodes under two different conditions. SEM displayed in Figure 6A is for poly(3-methylthiophene) formed by repeatedly cycling the potential of the microelectrode between  $-0.20$  V and  $1.65$  V, while that shown in Figure 6B for the electrode formed by applying a constant potential of  $1.65$  V. The film formed under repeated cycling looks more compact and has a “defined” apparent surface area, while that formed by applying constant potential to the microsubstrate showed scattering of the exposed surface of the polymer surface. This could be an explanation to the “ill-defined” response of the electrode as shown in the data of Figure 5B.

## 4. Conclusions

In summary, this work showed that it is possible to deposit conducting polymer films on microsize substrates of platinum. The electrochemical response of the conducting polymer microsize electrode is a function of the method used for electropolymerization. Better resolution for the determination of mixtures of biological compounds were obtained at polymer films formed by cycling the substrate between two potential limits of  $-0.2$  V

Table 2. Comparison between “micro” and “conventional” size conducting polymer electrodes [d] performance for the analysis of some organic molecules of biological interest.

| Analyte [a]    | Polymer microelectrode [b] |                         | Conventional polymer electrode [c] |                         |
|----------------|----------------------------|-------------------------|------------------------------------|-------------------------|
|                | Anodic                     | Cathodic                | Anodic                             | Cathodic                |
| Epinephrine    | 634 [mV]<br>3.983 E-6 A    | 465 [mV]<br>1.620 E-6 A | 627 [mV]<br>8.285 E-5 A            | 469 [mV]<br>4.490 E-5 A |
| L-Dopa         | 576<br>7.964 E-6           | 509<br>5.664 E-6        | 584<br>7.023 E-5                   | 495<br>5.489 E-5        |
| Norepinephrine | 617<br>4.392 E-6           | 473<br>1.976 E-6        | 623<br>6.582 E-5                   | 462<br>2.855 E-5        |
| Dopamine       | 552<br>4.795 E-6           | 493<br>3.977 E-6        | 563<br>1.014 E-4                   | 488<br>9.037 E-5        |
| Catechol       | 567<br>5.423 E-6           | 485<br>3.758 E-6        | 562<br>8.074 E-5                   | 485<br>7.141 E-5        |
| Hydroquinone   | 379<br>4.307 E-6           | 471<br>4.807 E-6        | 380<br>6.451 E-5                   | 471<br>4.846 E-5        |
| Ferricyanide   | 422<br>4.569 E-6           | 361<br>5.197 E-6        | 417<br>3.491 E-5                   | 355<br>3.165 E-5        |
| Ascorbic Acid  | 450<br>4.185 E-6           | –                       | 448<br>3.511 E-5                   | –                       |
| p-Aminophenol  | 529<br>8.473 E-6           | 495<br>3.855 E-6        | 534<br>6.657 E-5                   | 487<br>6.050 E-5        |
| Acetaminophen  | 690<br>8.288 E-6           | –                       | 695                                | –<br>7.144 E-5          |

[a] Analyte concentration: 5 mM in 0.1 M H<sub>2</sub>SO<sub>4</sub>; [b] Electrode diameter 8 μm; [c] Electrode diameter 3 mm; [d] Film formed upon cycling the electrode for 10 cycles in the monomer containing solution between +1.70 V and –0.120 V (vs. Ag/AgCl).

and +1.65 V (vs. Ag/AgCl). The electrochemical data at the polymer microelectrode were comparable to those obtained at “conventional”-size polymer electrodes. We concluded that, the electrochemical response is predominantly at the polymer electrolyte interface [21, 22]. The SEM results revealed the morphological differences between electrodes formed under applied constant potential and those deposited by cycling the potential at the substrate. Andrieux et al. [23] noticed that the dependence on the scan rate peak potentials and currents was a function of the polymeric system and its morphology. Our finding proves that the morphology of the polymer surface deposited at a microsize substrate affects the resolution of the three component system as indicated in Figure 5.

## 5. Acknowledgements

The author would like to thank the council of research and the University of United Arab Emirates for partial financial support. We are also indebted to Prof. J. F. Boerio and the University of Cincinnati for using the surface facilities. The author would like to thank the University of Cairo, Egypt for granting a leave of absence.

## 6. References

- [1] *Handbook of Conducting Polymers*, Vol. 1, 2 (Ed: T.A. Skotheim), Marcel Dekker, New York **1986**.

- [2] *Organic Electrochemistry, an Introduction and a Guide* (Eds: M.M. Baizer, H. Lund), Marcel Dekker, New York **1996**.
- [3] A. Dall'Olio, G. Dascola, V. Varacca, V. Bocchi, *Comptes Rendus* **1968**, C267:433.
- [4] A.G. MacDiarmid, A.J. Heeger, in *Molecular Materials* (Ed: W.E. Hatfield), Plenum, New York **1979**.
- [5] A.F. Diaz, K.K. Kanazawa, G.P. Gardini, *J. Chem. Soc. Chem. Comm.* **1979**, 635.
- [6] H.D. Abruña, in *Electroresponsive Molecular and Polymeric Systems*, Vol. 1 (Ed: T.A. Skotheim), Marcel Dekker, New York **1988**.
- [7] A. Ivaska, *Electroanalysis* **1991**, 3, 247.
- [8] H.B. Mark, Jr., N. Atta, Y.L. Ma, K.L. Petticrew, H. Zimmer, Y. Shi, S.K. Lunsford, J.F. Rubinson, A. Galal, *Bioelectrochem. Bioelectron.* **1995**, 38, 229.
- [9] R.M. Wightman, *Anal. Chem.* **1981**, 53, 1125A.
- [10] M. Fleischmann, S. Pons, D. Rolison, P.P. Schmidt, *Ultramicroelectrodes* Datatech Science, Morganton, NC **1987**.
- [11] M.A. Dayton, A.G. Ewing, M.R. Wightman, *Anal. Chem.* **1980**, 52, 2392.
- [12] C.P. Andrieux, P. Audebert, P. Hapiot, M. Nechtschein, C. Odin, *J. Electroanal. Chem.* **1991**, 305, 153.
- [13] R. John, G.G. Wallace, *J. Electroanal. Chem.* **1991**, 306, 157.
- [14] L.M. Abrantes, J.C. Mesquita, M. Kalaji, L.M. Peter, *J. Electroanal. Chem.* **1991**, 307, 275.
- [15] G. Tourillon, F. Garnier, *J. Electroanal. Chem.* **1982**, 135, 173.
- [16] J. Heinze, *Angew. Chem. Int. Engl.* **1993**, 32, 1268.
- [17] R.N. Adams, in *Electrochemistry at Solid Electrodes*, Marcel Dekker, New York **1969**.
- [18] N.F. Atta, A. Galal, A.E. Karagozler, G.C. Russell, H. Zimmer, H.B. Mark, Jr., *Biosens. Bioelectron.* **1991**, 6, 333.
- [19] G. Tourillon, F. Garnier, *Mol. Cryst. Liq. Cryst.* **1985**, 121, 349.
- [20] A. Galal Abdo, *Ph.D. Thesis*, University of Cincinnati, Cincinnati, OH **1992**.
- [21] J. Wang, R. Li, *Anal. Chem.* **1989**, 61, 2809.
- [22] A. Galal, *J. Solid State Electrochem.* **1997** in press.
- [23] C.P. Andrieux, P. Audebert, P. Hapiot, M. Nechtstein, C. Odin, *J. Electroanal. Chem.* **1991**, 305, 153.